Supplementary Information for

Hypoxia Evaluation in Xenograft Tumors by Cherenkov-Excited Luminescence Imaging during Radiotherapy

Xu Cao[1,2*], Srinivasa Rao Allu[3,4], Shudong Jiang[1,5], Jason R. Gunn[1], Cuiping Yao[1,6], Xin Jing[1,6], Petr Bruza[1], David J. Gladstone[1,5,7], Lesley A. Jarvis[5,7], Jie Tian[2,8], Harold M. Swartz[9], Sergei A. Vinogradov[3,4], and Brian W. Pogue[1,5]*

[1]Dartmouth College, Thayer School of Engineering, Hanover, New Hampshire, USA
[2]Xidian University, Engineering Research Center of Molecular & Neuroimaging, Ministry of Education, School of Life Science and Technology, Xi'an, Shaanxi, China
[3]Department of Biochemistry and Biophysics, Perelman School of Medicine, University of Pennsylvania, Philadelphia, PA, USA.
[4]Department of Chemistry, School or Arts and Sciences, University of Pennsylvania, Philadelphia, PA, USA.
[5]Norris Cotton Cancer Center, Dartmouth-Hitchcock Medical Center, Lebanon, NH, USA.
[6]Xi'an Jiaotong University, Institute of Biomedical Analytical Technology and Instrumentation, School of Life Science and Technology, Key Laboratory of Biomedical Information Engineering of Ministry of Education, Xi'an, Shaanxi, China
[7]Department of Medicine, Geisel School of Medicine, Dartmouth College, Hanover, New Hampshire, USA.
[8]CAS Key Laboratory of Molecular Imaging, Institute of Automation, Chinese Academy of Sciences, Beijing, China.
[9]Department of Radiology, Geisel School of Medicine, Dartmouth College, Hanover, New Hampshire, USA.

***Correspondence addressed to:**

Brian W. Pogue, Ph. D : Phone: (603) 646-3861 **Email:** brian.w.pogue@dartmouth.edu
Or
Xu Cao, Ph.D. Xu.Cao@Dartmouth.edu

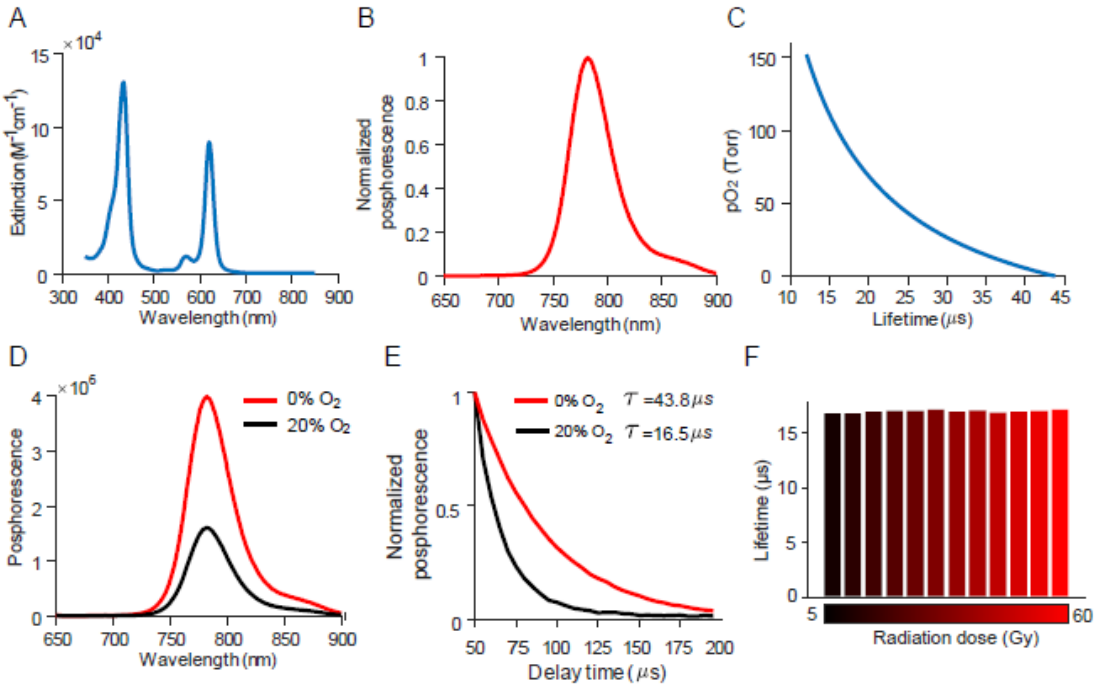

Fig. S1. Properties of Oxyphor PtG4. (A) Absorption spectrum of Oxyphor PtG4. (B) Emission spectrum of Oxyphor PtG4. (C) The pO2 values versus phosphorescent lifetime of Oxyphor PtG4. (D) The phosphorescent intensities of Oxyphor PtG4 under different oxygen levels. (E) The phosphorescent lifetimes of Oxyphor PtG4 under different oxygen levels. (F) The stability of Oxyphor PtG4 under irradiation by 6 MV X-ray beams.

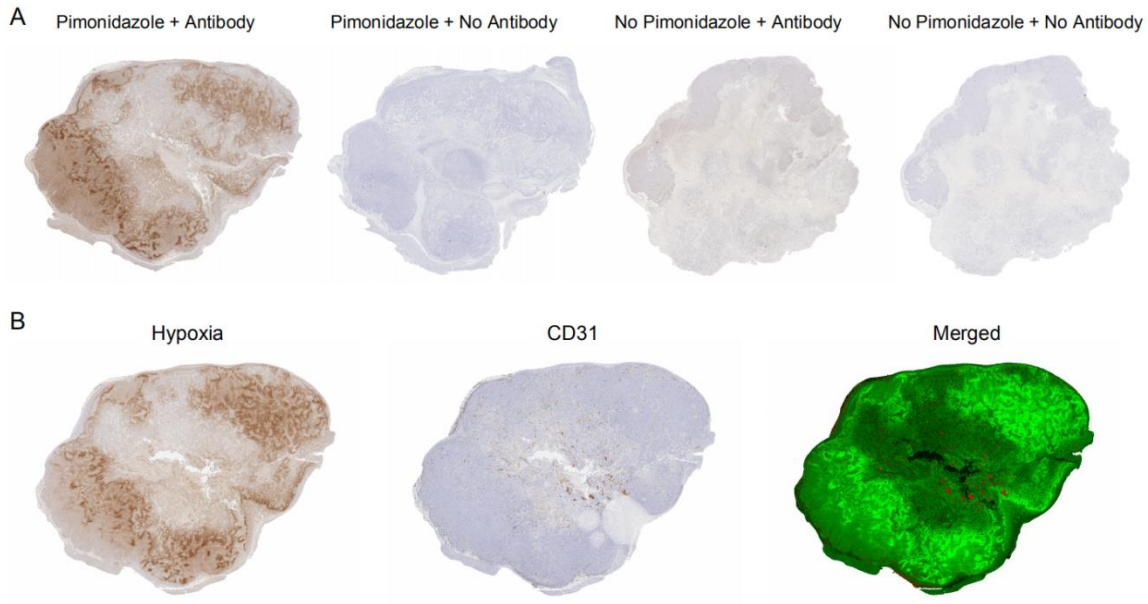

Fig. S2. Immunohistochemical staining for pimonidazole. (A) Validation of pimonidazole staining. Two tumors with and without administration of pimonidazole were cut and stained with and without anti-pimonidazole antibody. (B) Comparison between pimonidazole and CD31 staining.

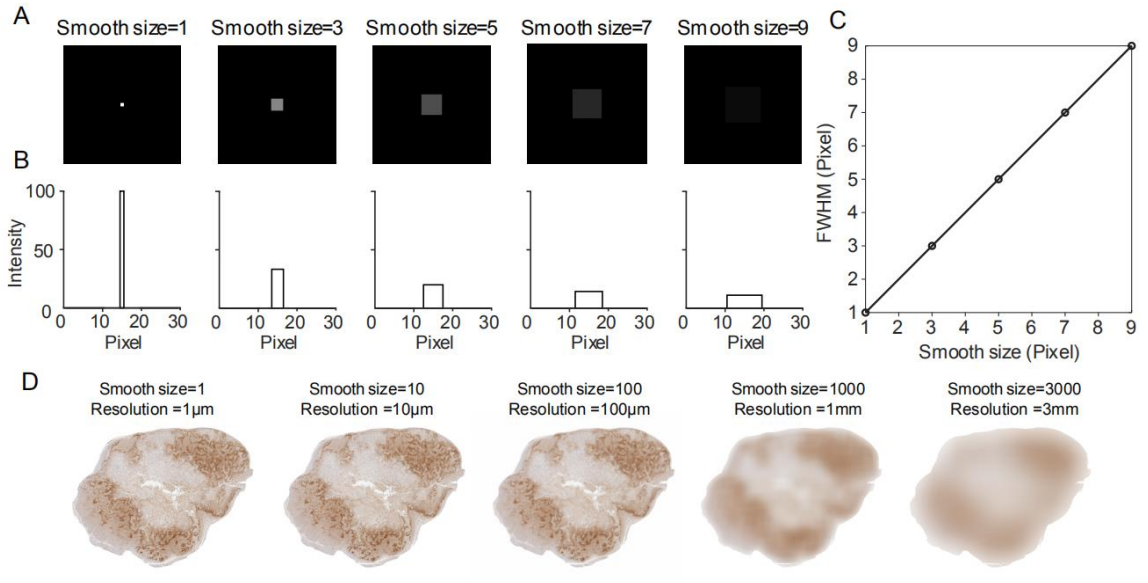

Fig. S3. Illustration of the resolution redaction of by smoothing process. (A) A simulated image with a single pixel was smoothed by using 2D mean filter with different smooth sizes. (B) Profile for each smoothed image in A to show its resolution defended by full width at half maximum (FWHM). (C) Resolution versus smooth size. (D) A example to show the resolutions reduction of a pimonidazole staining after smoothing with different smooth sizes.

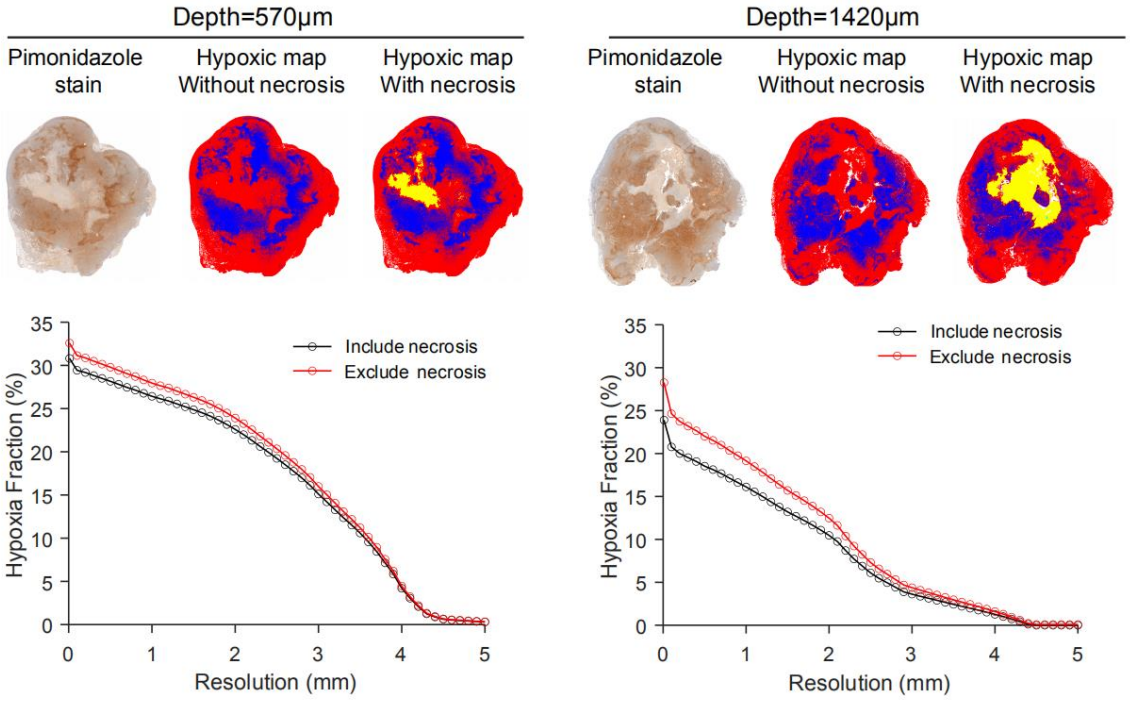

Fig. S4. Hypoxic fraction analysis excludes necrosis area. Two tumor sections were extracted from the same tumor at different depths with small (left panel) and large (right panel) necrosis areas (marked as yellow color). After removing the necrosis area from the nomaxic area (marked as red color), the hypoxic fraction (defined by the ratio of hypoxic area marked as blue to the sum of nomaxic and hypoxic areas) increased a little, but the tendency remains the same.

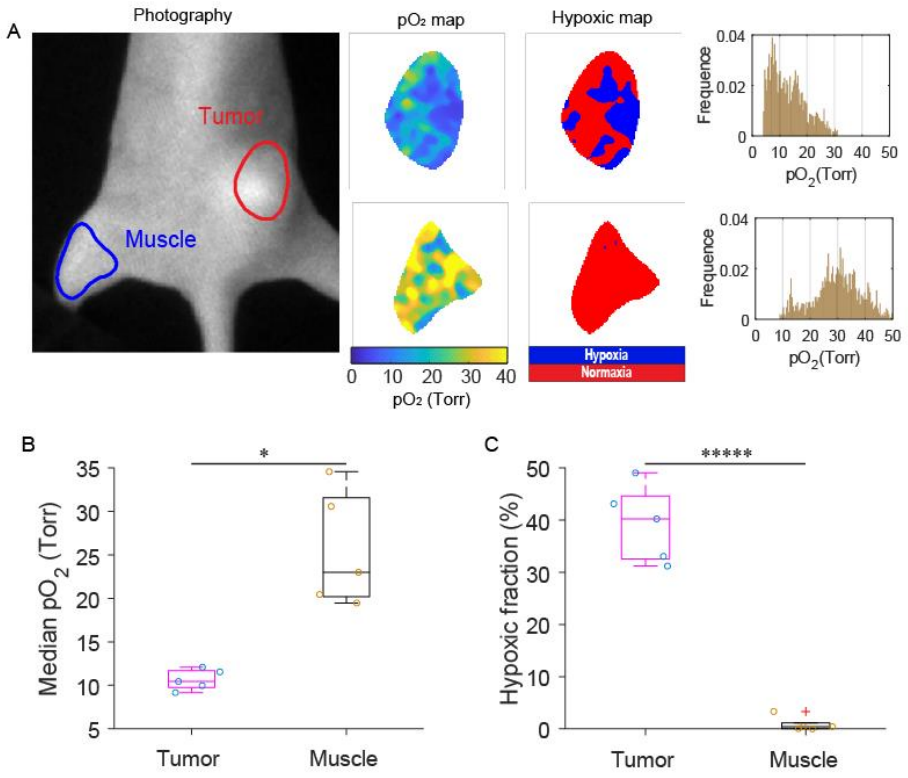

Fig. S5. CELI of oxygen in tumors and muscle *in vivo*. (A) Photography, pO2 maps, hypoxic maps and histograms for the MDA-MB-231 tumor (red circle) and muscle (blue circle). Oxyphor PtG4 was locally injected into the tumor and muscle a half hour before performing CELI. (B, C) Median pO2 (B) and hypoxic fraction (C) for the tumor and muscle (n=5 mice). Boxplot shows median and interquartile range, whiskers indicate the range. Two-sample t-test was used for statistical analysis. *P < 0.01, *****P < 0.0000001.

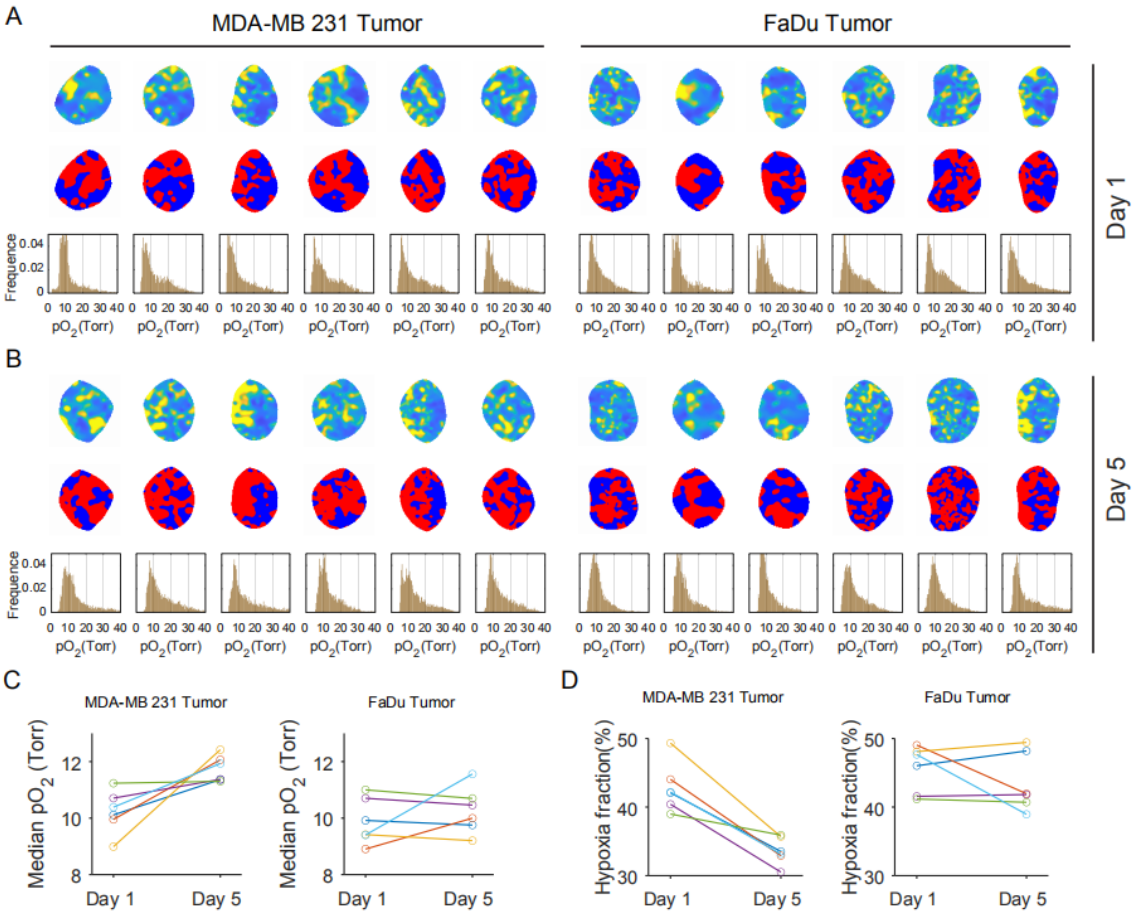

Fig. S6. In-vivo pO2 imaging of 12 mice (6 MDA-MB-231 and 6 FaDu tumors). (A, B) are pO2 maps, hypoxic maps and histograms for MDA-MB-231 and FaDu tumors on the first day (A) and the fifth day (B). (C, D) are comparison in median pO2 and hypoxic fraction between the first day and the fifth day.

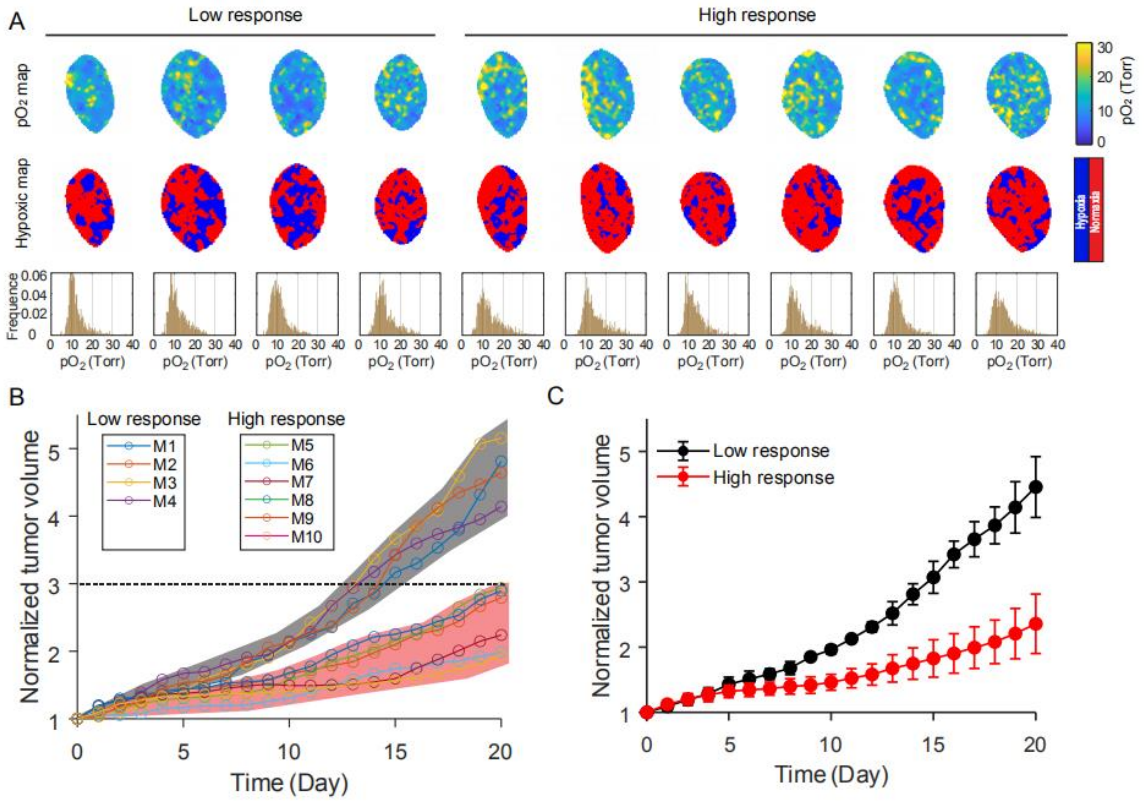

Fig. S7. In-vivo pO2 imaging of 10 mice with MDA-MB-231 tumor. (A) The pO2 maps, hypoxic maps and histograms for MDA-MB-231 tumors. (B) The relative tumor volume growth after the radiotherapy was normalized by the pre-treatment volume. The 10 tumors were divided into low response and high response to radiotherapy by the final growth ratio with a threshold of 3. (C) The relative tumor volume growth for low and high response to radiotherapy. The graph indicated mean $\pm$ Std.